

Radiative decay and phonon scattering of biexcitons in CuCl

H. Akiyama

Department of Physics, Faculty of Science, The University of Tokyo, 7-3-1 Hongo, Bunkyo-ku, Tokyo 113, Japan

T. Kuga and M. Matsuoka

The Institute for Solid State Physics, The University of Tokyo, 7-22-1 Roppongi, Minato-ku, Tokyo 106, Japan

M. Kuwata-Gonokami

Department of Applied Physics, Faculty of Engineering, The University of Tokyo, 7-3-1 Hongo, Bunkyo-ku, Tokyo 113, Japan

(Received 3 April 1990)

We have studied the spectra and the temporal behavior of the emissions from biexcitons in CuCl at 4–65 K created via two-photon absorption under weak-excitation conditions using high-repetition-rate (82-MHz) picosecond tunable uv light. Temperature dependences of the interband- and the intraband-relaxation rate of the biexciton are obtained. These relaxations are ascribed to radiative decay to excitons and to single-acoustic-phonon scattering, respectively. It is found that the radiative lifetime of the biexciton is short, 50 ps, and its deformation potential is small, 0.72 eV.

A biexciton^{1,2} is a bound state of two electrons and two holes. It is often described approximately as a bound state of two excitons, where the interaction between the excitons is treated as a perturbation. This approximation is justified if the binding energy of the biexciton (the energy difference between the two excitons and the biexciton) is much smaller than that of the exciton. If this is the case, the relaxation process of the biexciton reflects various features of exciton relaxation. Radiative decay of the biexciton is then described as an annihilation of one of the two excitons in it. It is very efficient because the annihilation can occur at any unit cell within the large orbitals of the biexciton. This is called the giant oscillator-strength effect.³ Phonons are supposed to interact with a biexciton as if they interact with two excitons in this perturbational treatment, where the change in the internal motion of the biexciton by lattice deformation, etc., is neglected.

CuCl is a prototypical material for the study of biexcitons,^{1,2} and the above picture holds well because the binding energy of the biexciton and that of the exciton are 32 (Ref. 4) and 190 meV (Ref. 5), respectively. Much work has been done so far on relaxation processes of biexcitons in CuCl. In most of these previous experiments, however, excitation light was so strong that various kinds of high-density excitation effects were induced, and the elementary relaxation process under weak-excitation conditions was not clear.

In the previous paper⁶ we reported the study of the dynamics of biexcitons in CuCl following the study of the excitonic polariton,^{7,8} and showed the importance of avoiding high-density excitation using weak picosecond pulses. The main results obtained at 4.2 K are as follows. First, the M emission lines (M_T , M_L , etc.), which appear when the biexcitons annihilate and leave excitons, are all very sharp, and no previously reported M bands appear. Second, the decay time of all these lines is shorter than the previously reported times, and it is about 30 ps.

In the present paper we extend the above study of the biexcitons to higher temperatures, and clarify the relaxation process resulted from the radiative decay and the biexciton-phonon interaction.

A platelet of CuCl single crystal with a thickness of 77 μm was held in a cryostat in a strain-free state and cooled directly by temperature-controlled helium-gas flow. The pulses from a cw mode-locked yttrium aluminum garnet (YAG) laser are frequency doubled in a KTP (KTiOPO₄) crystal to pump a tunable dye (Rhodamine-6G) laser. The transmitted YAG-laser pulses from the doubling crystal and the pulses of the dye laser are mixed in a BBO ($\beta\text{-BaB}_2\text{O}_4$) crystal to generate uv pulses. The output uv pulses have a repetition rate, 82 MHz, an average power, 4 mW, a pulse duration, 8 ps, and a spectral width, 2 meV. They were focused on the sample with a spot size of about 50 μm in diameter. The photon energy of the excitation light was tuned to the half of the biexciton energy to create biexcitons via two-photon absorption. The emitted light was collected with a lens in the backward-scattering geometry, and was directed towards a 50-cm monochromator. We measured time-integrated spectra with a photomultiplier and temporal responses with a synchroscan streak camera set behind the monochromator. A full width at half maximum (FWHM) of the observed temporal profile of the excitation light was typically 20 ps, which indicates the time resolution of the system.

Figure 1 shows the time-integrated emission spectra of CuCl under the excitation at the two-photon resonance to the biexciton energy. The excitation is weak enough and there are no higher-order nonlinear effects.⁶ We kept the excitation photon energy tuned to the resonance energy at each temperature, as is indicated by an arrow in the figure. At low temperatures, sharp lines, denoted M_L and M_T , are dominant. These two lines come from the photoemission of biexcitons which are not distributed in the momentum space before they radiate. As we raise the

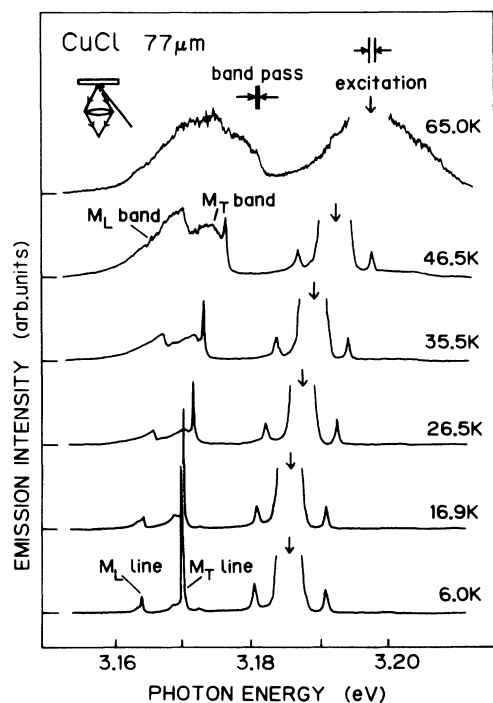


FIG. 1. Time-integrated backward-emission spectra of CuCl at various temperatures under the excitation at the two-photon resonance of the biexciton energy. The sharp lines (M_T and M_L lines) represent the radiative decay of biexcitons conserving their initial wave vector, and the broad bands (M_T and M_L bands) that of widely distributed biexcitons in momentum space scattered by acoustic phonons.

temperature, broad bands, denoted by M_L and M_T , appear and grow larger and broader. They originate from the biexcitons distributed in the momentum space due to scattering, most likely, by phonons. Since the translational mass of a biexciton is about twice as large as that of an exciton, the energy difference between the two states varies with momentum. Therefore, the distribution in momentum space gives rise to M_L and M_T bands. We can calculate⁹ the line shapes of the M_L and M_T bands to fit the data assuming vertical transitions. This analysis shows that the effective temperature of the distributed biexcitons is almost equal to the lattice temperature at all of the temperatures. This supports our assignment that the biexcitons are distributed in momentum space due to scattering by phonons.

Now we assume an intraband-relaxation rate, Γ_m , and an interband-relaxation rate, γ_m , as shown in Fig. 2. The biexcitons having the wave vector $2\mathbf{k}_0$ are created via two-photon absorption, where \mathbf{k}_0 is the wave vector of the excitation light in the crystal. Some of them are scattered to the states with different wave vectors $\mathbf{k} \neq 2\mathbf{k}_0$ with the rate Γ_m , and the others are not scattered before they make a transition to the lower bands with the rate γ_m . Based on this simple model, the evolution of the biexciton population after short-pulse excitation can easily be calculated. The population of the biexcitons at $\mathbf{k} = 2\mathbf{k}_0$, which contributes to the M_T line, decreases

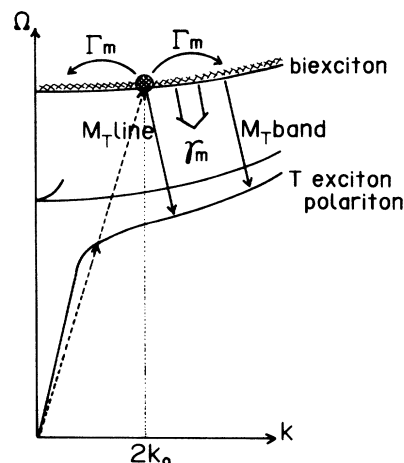


FIG. 2. Schematic dispersion curve of the biexciton and exciton bands. The dashed line represents the excitation of biexcitons with wave vector $2\mathbf{k}_0$ via two-photon absorption. The decays labeled " M_T line" and " M_T band" are radiative decays from the biexcitons before being scattered and after being scattered in the band, respectively. Γ_m is the intraband-relaxation rate, or the scattering rate. γ_m is the interband-relaxation rate, or the population-decay rate.

by $\exp[-(\gamma_m + \Gamma_m)t]$. The population at $\mathbf{k} \neq 2\mathbf{k}_0$, which contributes to the M_T band, varies as $[1 - \exp(-\Gamma_m t)]\exp(-\gamma_m t)$, so that, by measuring time traces of the M_T line and the M_T band, we can derive the interband- and intraband-relaxation rates.

We have measured the time dependences of the M_T -line and M_T -band intensities at various temperatures. As an example, a result at 19.8 K is shown in Fig. 3. The

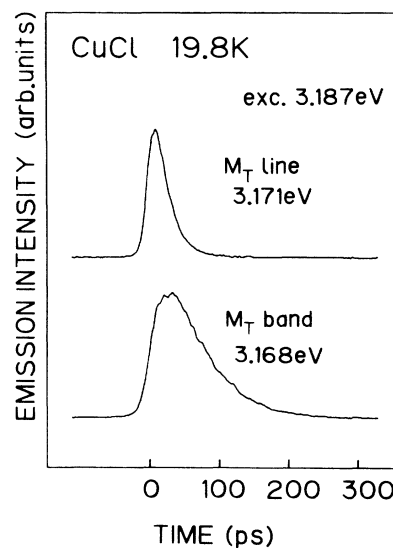


FIG. 3. Time trace of M_T -line and M_T -band intensities at 19.8 K measured in the backward-scattering geometry with a synchroscan streak camera. The decay rate of the M_T line is the sum of the interband- and intraband-relaxation rates of the biexciton, and that of the M_T band shows the interband-relaxation rate.

M_T line shows fast decay, which corresponds to the sum of the interband- and intraband-relaxation rates, $\gamma_m + \Gamma_m$. The M_T band shows a slow rise and slow decay. The decay represents the interband-relaxation rate γ_m .

Figure 4 is a plot of the inverse of the decay-time constants thus measured at various temperatures. Solid circles represent the decay rates of the M_T line, $\gamma_m + \Gamma_m$, and open circles those of the M_T band, γ_m . The decay rate of the M_T line above 40 K cannot be obtained because it is faster than the time resolution. The interband-relaxation rate γ_m is almost independent of temperature, and is about $1/(50 \text{ ps})$. This means that it does not represent the thermal-activation-type nonradiative relaxation. We ascribe the relaxation to radiative relaxation and the value 50 ps to the radiative lifetime of biexcitons. As to the intraband-relaxation rate Γ_m , it increases as the temperature rises. We assign its origin to scattering by one acoustic phonon.

The intraband-relaxation rate of a biexciton near $\mathbf{k}=0$ by means of single-acoustic-phonon scattering is given as follows:^{9,10}

$$\Gamma_{ac}(T) = (2/\pi)g_{mol}k_B T_1 / [\exp(T_1/T) - 1], \quad 0 < T \lesssim T_2 \quad (1)$$

where

$$T_1 = 2m_{mol}u^2/k_B, \quad T_2 = 2.6m_{mol}u^2/k_B g_{mol},$$

and

$$g_{mol} = (m_{mol}E_d^{mol})^2 / \hbar^3 \rho u.$$

Here, g_{mol} is the biexciton-acoustic-phonon coupling constant, E_d^{mol} the absolute value of the deformation potential for the biexciton, m_{mol} ($=5.29m_0$) (Ref. 11) the translational effective mass of the biexciton (m_0 is the free-electron mass), u ($=3.6 \times 10^5 \text{ cm/s}$) (Ref. 12) the ve-

locity of sound, and ρ ($=4.16 \text{ g cm}^{-3}$) (Ref. 13) the density of the crystal. As shown in Fig. 4, the function $\Gamma_0 + \Gamma_{ac}(T)$ expressed by the solid curve fits the solid circles well by assuming $g_{mol}=0.0175$ and $\Gamma_0=0.0145 \text{ meV}$, which gives $E_d^{mol}=0.72 \text{ eV}$ and $T_2=670 \text{ K}$ ($T_1=9.0 \text{ K}$).

As stated in the introductory part of this paper, phonons are supposed to interact with the biexciton as if they are interacting with two excitons, so that $E_d^{mol}=2E_d$ should hold approximately, where E_d is the deformation potential of an exciton. Anthony *et al.*¹⁴ measured it directly as the hydrostatic-pressure shifts of the $Z_{1,2}$ and Z_3 exciton absorption peaks, and obtained $E_d=0.4 \text{ eV}$. Masumoto and Shinonoya¹⁵ also reported $E_d=0.42 \text{ eV}$ by analyzing their experiment on the transient-induced absorption of picosecond pulses via the transition from excitons to biexcitons. The above-obtained value of E_d^{mol} is about twice these values, as expected. We note that these values of E_d and E_d^{mol} of CuCl are very small and that the phonon-scattering rate is very slow.

When Toyozawa's theory^{10,16} of the absorption line shapes of excitons interacting with acoustic phonons is applied to the two-photon-absorption line shape of biexcitons,⁹ we obtain an expression for the linewidth (FWHM),

$$W_{ac}(T) = \begin{cases} (2/\pi)g_{mol}k_B T_1 / [\exp(T_1/T) - 1], & 0 < T \lesssim T_2 \\ 0.3g_{mol}^2(k_B T)^2 / m_{mol}u^2, & T_2 < T \end{cases} \quad (2)$$

$$(3)$$

These expressions imply the following. At low temperatures, collisions with single phonons are well separated in time from each other (single-phonon scattering); therefore the absorption linewidth given by Eq. (2) is equal to the one-phonon-scattering rate given by Eq. (1). At high temperatures the phonon scatterings are so frequent that within the duration of one scattering other ones begin. A biexciton is always interacting with several phonons (multiple-phonon scattering). In this case, the biexciton states having different wave vectors intermingle with each other to give the linewidth given by Eq. (3).

Our result, $E_d^{mol}=0.72 \text{ eV}$ and $T_2=670 \text{ K}$, indicates that the coupling between the biexciton and the acoustic phonon is so small that the acoustic-phonon scatterings are always accounted for by single-phonon scatterings at all temperatures where the biexcitons can exist (0–80 K).

Itoh *et al.*⁹ measured the temperature dependence (0–80 K) of the linewidth (FWHM) of the two-photon absorption of the biexciton using a nitrogen-laser-pumped dye laser. They explained their experimental data in the high-temperature region ($T \gtrsim 50 \text{ K}$) with Eq. (3) assuming $g_{mol}=0.23$ ($E_d=2.6 \text{ eV}$, $T_2=50 \text{ K}$), and concluded that multiple-acoustic-phonon scattering is dominant above 50 K. This is not in agreement with our result. We propose another analysis of their data. In our analysis we consider the fact that the scattering by optical phonons ($\hbar\omega_{LO}=25.9 \text{ meV}$) (Ref. 17) becomes important at high temperatures, and it contributes to the width as¹⁰

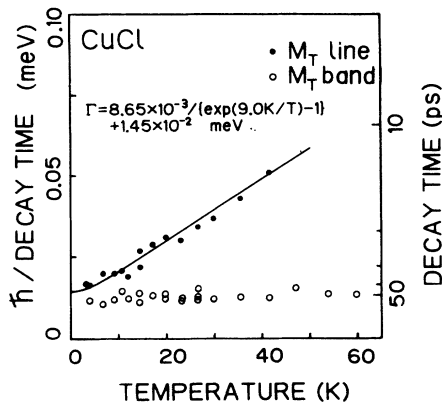


FIG. 4. Plot of the inverse of the decay-time constants of the M_T lines (solid circles) and M_T bands (open circles) as a function of temperature. The decay-time constants of the M_T bands do not depend on temperature and are about 50 ps, which is the radiative lifetime of the biexciton. The solid curve is a theoretical fit to the solid circles for single-acoustic-phonon scattering, where the deformation potential is assumed to be 0.72 eV.

$$W_{\text{op}}(T) = F / [\exp(\hbar\omega_{\text{LO}}/k_B T) - 1],$$

and we also consider the fact that, when the nanosecond-pulse laser is used, the excitons easily accumulate after M emission and collide with the biexcitons.⁶ Assuming that this gives the additional width W_{ex} , and neglecting its temperature dependence, we can analyze the data of Ref. 9 by writing the width $W = W_{\text{ac}}(T) + W_{\text{op}}(T) + W_{\text{ex}}$. We then obtain a better fit with $g_{\text{mol}} = 0.07$, $F = 83$ meV, and $W_{\text{ex}} = 0.26$ meV. This value of g_{mol} gives $E_d^{\text{mol}} = 1.4$ eV and $T_2 = 170$ K, which is now closer to our result. Possible errors in g_{mol} or E_d^{mol} in this analysis are large because W_{ac} is small compared to W_{ex} and W_{op} . We may say that the result of the experiment of Ref. 9 is consistent with that of our experiment. Therefore we can conclude that the single-acoustic-phonon scattering is dominant in the intraband relaxation at low temperatures, but optical-phonon scattering becomes dominant at high temperatures ($T \gtrsim 50$ K).

The radiative lifetime of 50 ps looks extraordinarily short, but this is explained by the giant oscillator-strength effect for the transition from a biexciton to an exciton, and it is expressed as^{18,19}

$$f_m/f_{\text{ex}} = 2 \left[\int g(\mathbf{R}) d\mathbf{R} \right]^2 / v.$$

Here, f_m is the oscillator strength for a biexciton, f_{ex} the oscillator strength for an exciton per primitive unit cell of the volume $v = (0.541 \text{ nm})^3/4$,²⁰ which can be evaluated from the LT (longitudinal-transverse energy) splitting, and $g(\mathbf{R})$ the wave function describing the relative motion of the two excitons in a biexciton. We can estimate²¹ the radiative lifetime of biexcitons in CuCl theoretically, assuming two types of wave functions for (a) the well-type and (b) the Coulomb-type binding potential as

$$g(\mathbf{R}) = (2\pi a_{\text{mol}})^{-1/2} R^{-1} \exp(-R/a_{\text{mol}}) \quad (4a)$$

and

$$g(\mathbf{R}) = (\pi a_{\text{mol}}^3)^{-1/2} \exp(-R/a_{\text{mol}}), \quad (4b)$$

where a_{mol} is determined from the experimental value of the binding energy. f_m/f_{ex} is then (a) 400 and (b) 3200, which leads to the radiative lifetime of (a) 470 and (b) 60 ps.

We have also made a similar calculation for (c) the Akimoto-Hanamura variational function,²²

$$g(\mathbf{R}) = C(\alpha R)^{\gamma/2} \exp(-\delta \alpha R/2), \quad (4c)$$

where C is a normalization factor. The variational calculation gives $\alpha = 0.93a_{\text{ex}}^{-1}$, $\delta = 1.04$, and $\gamma = 2.0$ for the mass ratio $m_e/m_h = 0.25$,²³ where $a_{\text{ex}} (= 0.70 \text{ nm})$ (Ref. 24) is the Bohr radius of an exciton. Our estimation gives

$$\frac{f_m}{f_{\text{ex}}} = \frac{\pi a_{\text{ex}}^3 2^{9+\gamma} [\Gamma(3+\gamma/2)]^2}{v \alpha^3 \delta^3 \Gamma(3+\gamma)} = 1.0 \times 10^5,$$

and a radiative lifetime of 2 ps, where $\Gamma(x)$ is the gamma function.

Although these wave functions are all good for evaluating the binding energy and the mean radius $\langle R \rangle$, they give quite different values for the radiative lifetime because it is more sensitive to the wave function $g(\mathbf{R})$. We can infer that, near $R \sim 0$, the wave function (4c) is the most appropriate one because this includes the effect of strong electron-electron and hole-hole correlations. At $R \sim \infty$, however, the wave function (4a) is better than (4b) or (4c), because the binding potential of two excitons is a short-range one. Theoretical evaluation of the radiative lifetime with enough accuracy requires full knowledge of $g(\mathbf{R})$, which is presently lacking, but the above examination makes us realize that 50 ps is a realistic value for the radiative lifetime of the biexcitons in CuCl.

From the measured lifetime of 50 ps, we can estimate the giant oscillator strength as

$$2 \left[\int g(\mathbf{R}) d\mathbf{R} \right]^2 / v = 4000.$$

This value is much larger than what was estimated from a measurement of the two-photon-absorption coefficient.²⁵ This is probably because⁶ the light pulses used in the experiment caused strong excitation effects, as was the case with previous lifetime measurements, etc. Thus, we may say that we successfully measured not only the lifetime, but also the quantitative value of the giant oscillator strength without strong excitation effects.

In conclusion, we have measured the temporal behavior of the M_T emissions from the biexcitons at various temperatures. We have obtained the temperature dependence of the interband- and intraband-relaxation rates of the biexcitons in CuCl under weak-excitation conditions. The temperature-independent interband relaxation is caused by the radiative decay to excitons, and the radiative lifetime is 50 ps. This short lifetime can be reasonably explained by the giant oscillator-strength effect. The intraband relaxation below 40 K is caused by single-acoustic-phonon scattering, and the deformation potential for biexcitons is 0.72 eV. Above 50 K the intraband relaxation is dominated by the optical-phonon scattering.

The authors would like to thank Professor Y. Toyozawa for theoretical suggestions about the phonon-scattering processes, Professor E. Hanamura for theoretical suggestions about the radiative decay processes of biexcitons, and Professor T. Itoh for valuable discussions. One of the authors (H.A.) would like to thank Professor T. Ninomiya for his continuous support of the present work.

¹M. Ueta, H. Kanzaki, K. Kobayashi, Y. Toyozawa, and E. Hanamura, *Excitonic Processes in Solids* (Springer-Verlag, Berlin, 1986).

²J. B. Grun, B. Hönerlage, and R. Lévy, in *Excitons*, edited by

E. I. Rashba and M. D. Sturge (North-Holland, Amsterdam, 1982).

³E. I. Rashba and G. E. Gurgenishvili, *Fiz. Tverd. Tela* (Leningrad) **4**, 1029 (1962) [*Sov. Phys—Solid State* **4**, 759 (1962)].

- ⁴G. M. Gale and A. Mysyrowicz, *Phys. Rev. Lett.* **32**, 727 (1974).
- ⁵A. Goldmann, *Phys. Status Solidi B* **81**, 9 (1977).
- ⁶H. Akiyama, M. Kuwata, T. Kuga, and M. Matsuoka, *Phys. Rev. B* **39**, 12 973 (1989).
- ⁷T. Kuga, M. Kuwata, H. Akiyama, T. Hirano, and M. Matsuoka, in *Ultrafast Phenomena VI*, edited by T. Yajima, K. Yoshihara, C. B. Harris, and S. Shionoya (Springer-Verlag, Berlin, 1988), p. 249.
- ⁸M. Kuwata, T. Kuga, H. Akiyama, T. Hirano, and M. Matsuoka, *Phys. Rev. Lett.* **61**, 1226 (1988).
- ⁹T. Itoh, S. Watanabe, and M. Ueta, *J. Phys. Soc. Jpn.* **48**, 542 (1980).
- ¹⁰Y. Toyozawa, *Prog. Theor. Phys.* **20**, 53 (1958).
- ¹¹T. Mita, K. Sôtome, and M. Ueta, *Solid State Commun.* **33**, 1135 (1980).
- ¹²R. C. Hansen, K. Helliwell, and C. Schwab, *Phys. Rev. B* **9**, 2649 (1974).
- ¹³T. H. K. Barron, J. A. Birch, and G. K. White, *J. Phys. C* **10**, 1617 (1977).
- ¹⁴J. B. Anthony, A. D. Brothers, and D. W. Lynch, *Phys. Rev. B* **5**, 3189 (1972).
- ¹⁵Y. Masumoto and S. Shionoya, *J. Phys. Soc. Jpn.* **51**, 181 (1982).
- ¹⁶Y. Toyozawa, *Prog. Theor. Phys.* **27**, 89 (1962).
- ¹⁷T. Nanba, K. Hachisu, and M. Ikezawa, *J. Phys. Soc. Jpn.* **50**, 1579 (1981).
- ¹⁸A. A. Golovin and E. I. Rashba, *Pis'ma Zh. Eksp. Teor. Fiz.* **17**, 690 (1973) [*JETP Lett.* **17**, 478 (1973)].
- ¹⁹E. Hanamura, *J. Phys. Soc. Jpn.* **39**, 1516 (1975).
- ²⁰J. N. Plendl and L. C. Mansur, *Appl. Opt.* **11**, 1194 (1972).
- ²¹M. Ojima, T. Kushida, Y. Tanaka, and S. Shinonoya, *J. Phys. Soc. Jpn.* **44**, 1294 (1978).
- ²²O. Akimoto and E. Hanamura, *J. Phys. Soc. Jpn.* **33**, 1537 (1972).
- ²³The effective masses of electrons and holes in CuCl are not fixed precisely, as shown in Ref. 1, p. 135. Here, we adopt an approximate value, which is enough for the estimation.
- ²⁴J. Ringeissen and S. Nikitine, *J. Phys. (Paris) Colloq.* **28**, C3-48 (1967).
- ²⁵V. D. Phach, A. Bivas, B. Hönerlage, and J. B. Grun, *Phys. Status Solidi B* **84**, 731 (1977).